

## Rare-Earth Oxide Substituted LiNbO<sub>3</sub> Nanopowders Obtained By Polymerizable Complex Method

Monica Popa and Masato Kakihana

Materials and Structures Laboratory, Tokyo Institute of Technology,  
Nagatsuta 4259, Midori-ku, Yokohama 226-8503, Japan  
Fax: +81 45 924 5309; email: [pmonica@msl.titech.ac.jp](mailto:pmonica@msl.titech.ac.jp)  
Email: [kakihana@msl.titech.ac.jp](mailto:kakihana@msl.titech.ac.jp)

Nanopowders of lithium niobate LiNbO<sub>3</sub> and rare earth (RE) Sm and Pr substituted LiNbO<sub>3</sub>,  $x \leq 0.05$ , were synthesized using a wet chemical method, the polymerizable complex method, based on the Pechini-type reaction route. A mixed solution of citric acid and ethylene glycol with Li, Nb and RE ions was polymerized. The formation, the homogeneity and the structure of the obtained powders have been investigated by Raman spectroscopy and scanning electron microscopy measurements. The X-ray diffraction analysis indicated the formation of perovskite-type oxides, which crystallized in the rhombohedral system when the Li-Nb and Li-Nb-RE polymeric precursors were treated at temperatures as low as 500°C for 2 h. No additional crystalline phases formed during calcination. Small, homogeneous particles in nanoscale range were obtained, with no significant particle growth till 700°C. The Raman spectroscopy data of LiNbO<sub>3</sub> substituted by RE ion were compared to the results of the un-substituted system.

Key words: LiNbO<sub>3</sub>; rare earth ion substitution; polymerizable complex method; nanopowders; Raman spectroscopy.

### 1. INTRODUCTION

Lithium niobate LiNbO<sub>3</sub> (referred to as LN) is a widely used material due to its large number of interesting properties: electro-optical, non-linear optical, ferroelectric, piezoelectric, pyroelectric; it is a very good candidate for optoelectronic devices as it has excellent electro-optic and acousto-optic coefficient [1-5]. The possibility of doping LiNbO<sub>3</sub> with active ions which can be lased in the visible and infrared region is a promising perspective in the investigation of optically active ions in LiNbO<sub>3</sub> [1, 6]. Rare earth ions have been introduced in LiNbO<sub>3</sub> matrix as they are well known laser ions in many other materials. Studies on Nd<sup>3+</sup>, Er<sup>3+</sup>, Dy<sup>3+</sup>, have been reported as well as Pr<sup>3+</sup>, Ho<sup>3+</sup>, Yb<sup>3+</sup> on single crystals of LiNbO<sub>3</sub> [1, 6-12]. Doping with foreign RE ions modifies the optical properties of the matrix and makes the system useful for many applications in optical devices: optical planar waveguides, phosphors, solid state lasers, sensors, holographic storage systems. In this respect LiNbO<sub>3</sub> is complicated as an impurity ion can be located in four different lattice sites; moreover, the rare earth ions are found to be surrounded by different crystalline environments (multi-centres), which additionally complicates the optical spectra [1]. These ions can be dispersed in non-equivalent local environments in the host crystal, giving place to different optical transitions. The distribution of the active ions in different centres can strongly affect their optical properties. Determination of the lattice location for the laser active ions therefore becomes of great importance.

Raman spectroscopy can be a sensitive tool for detecting small changes in the structure through lattice deformations of LN. Defects and impurities can lead to frequency shifts or broadening of Raman lines [13]. Raman spectra for LN doped materials are incompletely

studied and although investigations are reported on these systems there still are discrepancies in the results.

Although LN is usually studied as single crystals or thin films, polycrystalline LN has also its important technological applications [5, 14]. Polymerized complex (PC) method was used for the synthesis of high pure multicomponent oxides because of its inherent advantages over other methods: better homogeneity, compositional control, lower processing temperatures resulting in more reactive powders [5, 15].

In our previous investigation we carried out research related to the synthesis and characterization performed in order to demonstrate the suitability and advantages of the PC method to provide homogeneous ceramic single-phase nanopowders of rare earth (RE) substituted lithium niobate oxides with perovskite structures at temperatures as low as 500°C. A study of the substitution effect on the lattice and the influence on the structure and properties was also discussed [5]. A part of the experimental results obtained from this research and a brief discussion are given in the present paper, referring mainly to the particle morphology and Raman analysis for a 2% molar ratio rare earth substitution of Li in LiNbO<sub>3</sub>. We have studied two rare-earth ions in LiNbO<sub>3</sub> and a comparison with previous data has been made [5].

### 2. EXPERIMENTAL

#### 2.1 Synthesis conditions

The synthesis procedure for powders of LiNbO<sub>3</sub>, as well as for RE ion substituted LiNbO<sub>3</sub> were outlined previously [5]. The materials used, as well as their origin are shown in Table I.

The starting materials were Li<sub>2</sub>CO<sub>3</sub> and Nb-ammonium complex which were dissolved in an aqueous solution of citric acid. The RE compounds La<sub>2</sub>O<sub>3</sub>•3H<sub>2</sub>O, Pr<sub>2</sub>(CO<sub>3</sub>)<sub>3</sub>,

Sm<sub>2</sub>(CO<sub>3</sub>)<sub>3</sub>, and Er<sub>2</sub>(CO<sub>3</sub>)<sub>3</sub> respectively, were added corresponding to 2% molar ratio substitution of Li in LiNbO<sub>3</sub>. Clear transparent solutions were obtained and ethylene glycol was added.

Table I. Materials used in the synthesis of LiNbO<sub>3</sub>, and RE ion substituted LiNbO<sub>3</sub>.

Material	Composition	Origin
Lithium carbonate	Li <sub>2</sub> CO <sub>3</sub>	Kanto Ch. Japan
Nb ammonium complex	NH <sub>4</sub> [NbO(C <sub>2</sub> O <sub>4</sub> ) <sub>3</sub> H <sub>2</sub> ] nH <sub>2</sub> O	CBMM Brazil
Citric acid (CA)	C <sub>6</sub> H <sub>8</sub> O <sub>7</sub>	Wako Ch. Japan
Ethylene glycol (EG)	C <sub>2</sub> H <sub>6</sub> O <sub>2</sub>	Kanto Ch. Japan
Lanthanum oxide	La <sub>2</sub> O <sub>3</sub> ·3H <sub>2</sub> O	Wako Ch. Japan
Praseodymium carbonate	Pr <sub>2</sub> (CO <sub>3</sub> ) <sub>3</sub> ·8H <sub>2</sub> O	Seimi Ch. Japan
Samarium carbonate	Sm <sub>2</sub> (CO <sub>3</sub> ) <sub>3</sub>	Seimi Ch. Japan
Erbium carbonate	Er <sub>2</sub> (CO <sub>3</sub> ) <sub>3</sub>	Seimi Ch. Japan

The solutions were continuously stirred and the temperature was slowly increased to remove the excess water and to accelerate the polyesterification reaction between CA and EG. Heating of the polymeric resin at high temperatures, above 300°C causes a breakdown of the polymer. The resulting resin was treated in a mantle heater at 400 ~ 450°C for over 3 h, to induce charring. The resulting material had the appearance of a dark brown sticky ash, which was slightly ground into a powder by a Teflon rod. The as-obtained powder is referred to as the "precursor" hereafter, and was heat-treated between 500°C and 900°C for 2 h.

## 2. 2 Characterization

The synthesized materials were characterized by thermal analysis and thermogravimetry (DTA/TG) and the products obtained during different stages were characterized by X-ray diffractometry (XRD) and Raman spectroscopy. The microstructure of the materials was evaluated by scanning electron microscopy (SEM). Phase purities and crystal structure of the obtained materials were determined by X-ray diffractometry. The patterns were recorded using CuK<sub>α</sub> radiation ( $\lambda=1.5405 \text{ \AA}$ ) at a scanning rate of 2°/min in the (2 $\theta$ ) range from 15° to 75°. The scanning electron microscopy was performed in a Hitachi S-4500 scanning microscope for particle morphology and microstructure of the samples. The Raman spectra were performed at room temperature by using a triple spectrometer Jobin Yvon/Atago-Bussan T-6400 with a liquid nitrogen cooled CCD detector for 800 s, in micro-mode. The Ar<sup>+</sup> laser beam with the excitation  $\lambda=514.5 \text{ nm}$  was focused under a 90x microscope objective and the laser spot size was between 1 ~ 2  $\mu\text{m}$ . Raman spectra were recorded in 1000-100  $\text{cm}^{-1}$  range. The spectral resolution was 1  $\text{cm}^{-1}$ .

## 3. RESULTS AND DISCUSSION

Complete crystallization of LiNbO<sub>3</sub> takes place at 700°C. The powder X-ray diffraction pattern of the

undoped material revealed that sample has a rhombohedral perovskite structure, with the average lattice parameters  $a=5.151 \text{ \AA}$  and  $c=13.832 \text{ \AA}$  [5].

Fine single-phase powders with particles in the nanoscale range were obtained at temperatures as low as 500°C. All powders presented similar structure with good homogeneity and uniform spherical grain size; there was no effect observed on the particle size for the rare earth ion doping. Figure 1 shows an example of the microstructure of LN containing 2% Pr prepared by the PC method obtained at 700°C. The mean particle size was between 60-70 nm. The SEM micrograph shows a uniform grain size distribution, a fine powder size and homogeneous microstructure. Increasing the calcination temperatures, sintering occurred in the samples but even after calcination at 900°C the particle size of the powders was around ~100-120 nm. Crystallization of nanopowders occurs at low temperature and the grain growth with increasing the calcination temperature is slow.

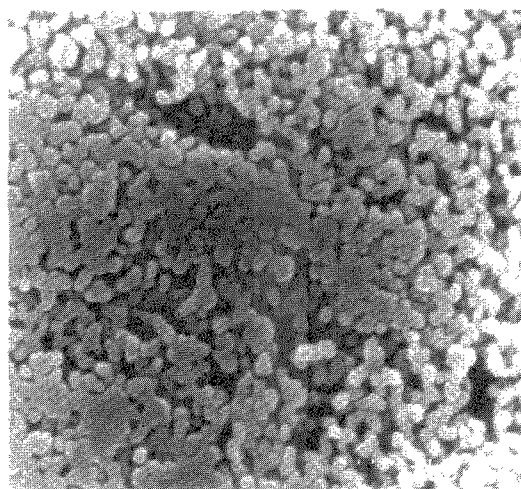


Fig. 1 SEM micrograph showing the particle size of Pr ion containing perovskite powders prepared by PC method treated at 700°C.

The chemical and microstructural homogeneity affects the electro-optic behaviour, therefore the synthesis of niobates with good stoichiometry, homogeneity and sinterability are very important for developing LiNbO<sub>3</sub> based ceramics. The small particle size and the homogeneity of the particles can be regarded as reasons for the high sinterability of our niobate powders.

At room temperature LN exhibits a ferroelectric rhombohedral structure belonging to the space group R3c (C<sub>3v</sub><sup>9</sup>), with the primitive cell containing two formula units. Consequently, 18 vibration modes should be expected and are divided into (4A<sub>1</sub>+9E+5A<sub>2</sub>) in which A<sub>2</sub> phonons are Raman and IR inactive, while A<sub>1</sub> and E are both Raman and IR active. We have performed Raman scattering measurements in the LN and LN containing RE samples. The phonon assignments were analysed in a previous work [5].

In Figure 2 the Raman spectra of RE-substituted LN are compared to the spectrum of pure LiNbO<sub>3</sub>. The mode frequencies in substituted powders are evaluated with respect of the values in un-substituted samples.

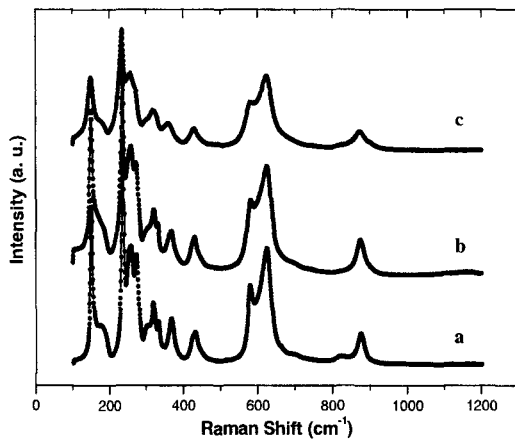


Fig. 2 The Raman spectra of RE ion (Pr-b and Sm-c) substituted LN are compared to the spectrum of pure  $\text{LiNbO}_3$ .

We analyse here the changes observed in the  $E(\text{TO}_1)$ ,  $E(\text{TO}_2)$ ,  $E(\text{TO}_3)$ ,  $E(\text{TO}_4)$ ,  $E(\text{TO}_5)$ ,  $A_1(\text{TO}_1)$ ,  $A_1(\text{TO}_2)$ ,  $A_1(\text{TO}_3)$ ,  $A_1(\text{TO}_4)$  phonon modes, shown in Figure 3. As it can be observed in both figures Fig. 2 and Fig. 3, there is an increase of damping in all the bands with the addition of RE ion in the composition.

As a general observation it seems that RE ions presence lowers the frequency and a shift of the bands take place with RE addition. The  $A_1(\text{TO}_2)$ ,  $A_1(\text{TO}_3)$  bands are significantly affected by doping. The  $A_1(\text{TO}_2)$  phonon shows a significant damping and shifts to lower frequency. If compared with the behaviour of the other phonons this band shows the most significant change. The  $A_1(\text{TO}_2)$  phonon is associated with the displacement of ions situated on A sites (the  $\text{Li}^+$  site) in antiphase to ions situated in B sites (the  $\text{Nb}^{5+}$  site) [7]. A similar discussion can be made regarding the behaviour of the  $A_1(\text{TO}_3)$  phonon mode, associated with the rotation of whole oxygen octahedra along the trigonal axis. Since the modes  $A_1(\text{TO}_2)$  and  $A_1(\text{TO}_3)$  exhibit the most significant changes in frequency and represent a substantial amount of Li movement in the A site, we can assume that RE ions are located at the A sites, which is in agreement with results published by Mouras et al [7] and Zhang et al [8] and also in agreement with our previous observations in the systems doped with higher content of RE [5].

On the other hand, the  $A_1(\text{TO}_1)$ ,  $E(\text{TO}_1)$ ,  $E(\text{TO}_5)$  phonon modes exhibit significantly lower shifting in frequency. These modes are associated with the movement in B sites of the perovskite lattice occupied by Nb atoms. The  $A_1(\text{TO}_1)$  mode represents the vibration of Nb atoms in antiphase with the oxygen plane along the trigonal axis and exhibits little shift in its Raman frequency, while the  $E(\text{TO}_1)$  mode represents the in-plane bending vibration of the oxygen octahedra in the plane perpendicular to the trigonal axis -the plane (x, y) of the  $\text{BO}_6$  ( $\text{NbO}_6$ ) octahedral. We have chosen  $E(\text{TO}_1)$  to investigate the effect of substitution in Nb sites, as this mode has nothing to do with the movement of Li ions [16].

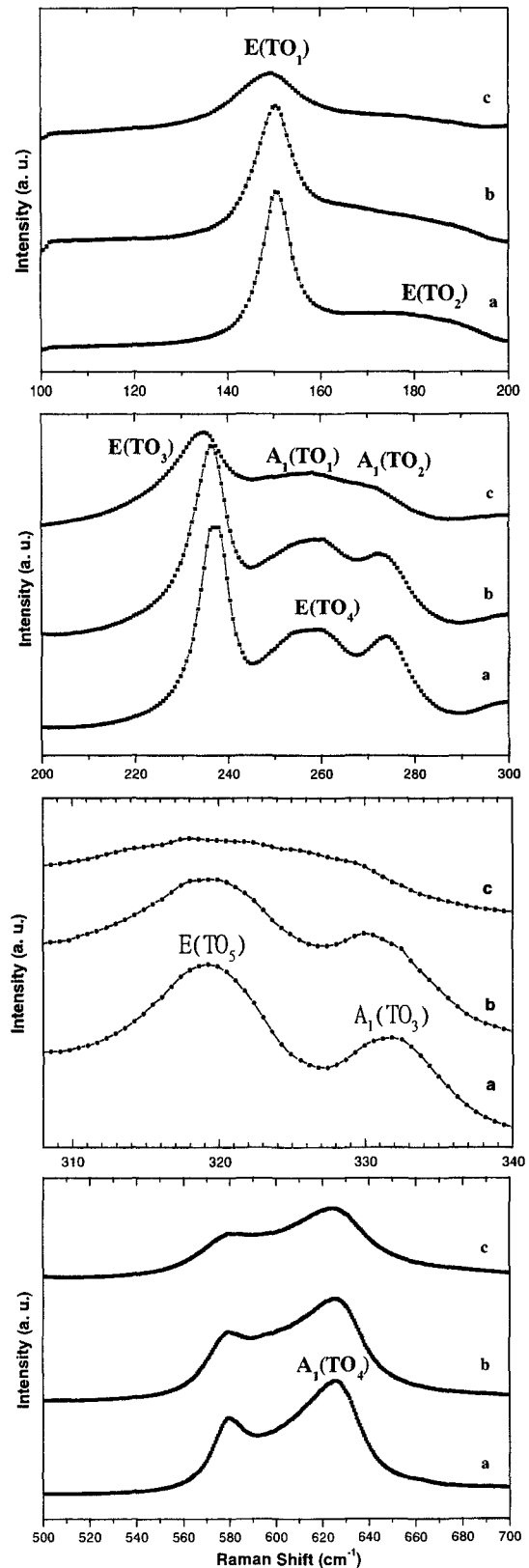


Fig. 3 The  $E(\text{TO}_1)$ ,  $E(\text{TO}_3)$ ,  $A_1(\text{TO}_3)$ ,  $A_1(\text{TO}_2)$ ,  $A_1(\text{TO}_3)$ ,  $A_1(\text{TO}_4)$  Raman bands obtained in LN containing Pr ion (b) and Sm ion (c) compared to pure  $\text{LiNbO}_3$  (a).

The effect of doping in the Raman bands associated with the movement of Nb and Li atoms is illustrated in Figure 4, where the evolution of the frequency for the  $E(\text{TO}_1)$  mode is shown, compared to the behaviour of the main bands associated to the movement of Li sites discussed above,  $A_1(\text{TO}_2)$ , and  $A_1(\text{TO}_3)$ .

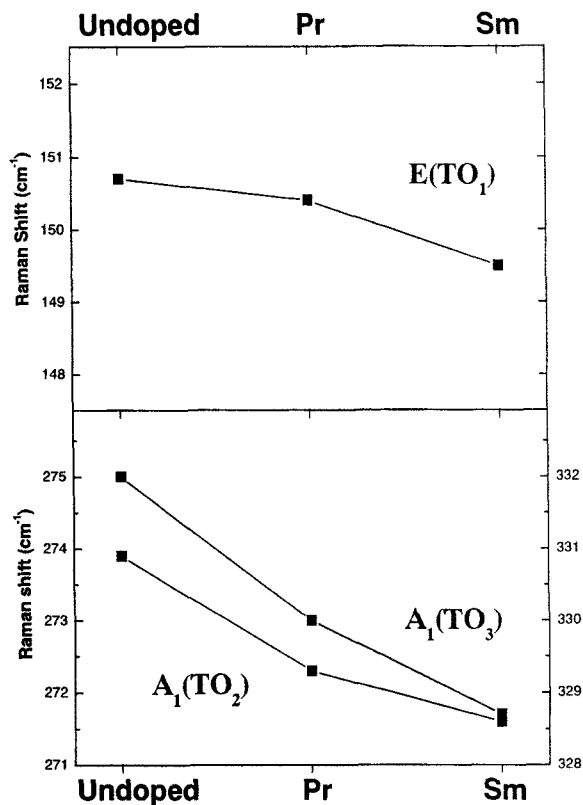


Fig. 4 Dependence of Raman shift on the Li ion substituted with 2% RE (Pr and Sm) ions for the  $E(\text{TO}_1)$ ,  $A_1(\text{TO}_2)$ ,  $A_1(\text{TO}_3)$  phonon modes.

There is a decrease in the Raman shift of the phonon modes  $A_1(\text{TO}_2)$  and  $A_1(\text{TO}_3)$  associated to the movement in Li sites both for the Pr and Sm substitution; the Pr presence does not seem to affect the Nb sites, while a small decrease of the intensity of the bands associated to the Nb atoms movement is noticed in the case of Sm substitution; Sm substitution seems to affect both the Li and Nb sites.

At this point, according to the Raman spectroscopy results and in agreement with previous reported results using this method of characterization and analysis [1, 3, 5, 7, 8, 17] it seems that clearly affected modes appear to be those related to the Li sites. Studies are underway in order to determine the  $\text{RE}^{3+}$  ions substitution influence on the properties and structure of LN.

#### 4. CONCLUSIONS

The polymerizable complex method has been used to provide very homogeneous, single-phase ultra-fine  $\text{LiNbO}_3$  and RE ion substituted  $\text{LiNbO}_3$  based powders. Crystallization of nanopowders occurs at  $500^\circ\text{C}$  and the grain growth with increasing the calcination temperature is slow. Even after calcination at  $900^\circ\text{C}$ , the particle size

of the powders was  $\sim 100$  nm which is the usual lowest limit of most common commercial powders.

The Raman spectroscopy results allowed us to assign and describe the vibrational modes in LN as well as to analyse the evolution of the modes in RE ion substituted LN. The  $A_1(\text{TO}_2)$ ,  $A_1(\text{TO}_3)$  and  $E(\text{TO}_2)$  were the modes which were most affected by the substitution, as the bands were shifted from their fundamental frequency in LN.

We demonstrated the effectiveness of Raman spectroscopy as an easy tool to determine the structural modifications induced by the substitution of Li ion in LN by  $\text{RE}^{3+}$ : Pr and Sm ions.

#### 5. REFERENCES

- [1] A. Lorenzo, H. Jaffrezic, B. Roux, G. Boulon and J. Garcia Sole, *Appl. Phys. Lett.* **67** (25), 3735-37 (1995).
- [2] C.D.E. Lakeman and D.A. Payne, *Mater. Chem. Phys.*, **38** (4), 305-24 (1994).
- [3] R. Mouras, S. M. Kostitskii, P. Bourson, M. Aillerie and M. D. Fontana, *Opt. Mater.*, **18**, 127-30 (2001).
- [4] S. Lanfredi and A. C. M. Rodrigues, *J. Appl. Phys.*, **86**, 2215-20 (1999).
- [5] M. Popa and M. Kakihana, *Cat. Today*, **2860**, 1-9, (2002).
- [6] L. F. Johnson and A. A. Ballman, *J. Appl. Phys.*, **40**, 297-302 (1969).
- [7] R. Mouras, P. Bourson, M. D. Fontana and G. Boulon, *Optics Commun.*, **197**, 439-44 (2001).
- [8] D. Zhang, X. Chen, Y. Wang, D. Zhu, B. Wu and G. Lan, *J. Phys. Chem. Solids*, **63**, 345-58 (2002).
- [9] E. Cantelar, J. A. Sanz-Garcia and F. Cusso, *J. Cryst. Growth*, **205**, 196-201 (1999).
- [10] C. Prieto, *Opt. Mater.*, **12**, 135-42 (1999).
- [11] C. Sada, F. Caccavale, F. Segato, B. Allieri, L. E. Depero, *Opt. Mater.*, **19**, 23-31 (2002).
- [12] J. Garcia Sole, L. E. Bausa, D. Jaque, E. Montoya, H. Murrieta and F. Jaque, *Spectr. Acta Part A*, **54**, 1571-81 (1998).
- [13] A. Ridah, P. Bourson, M. D. Fontana and G. Malovichko, *J. Phys. Condens. Matter.*, **9**, 9687-93 (1997).
- [14] E. Camargo and M. Kakihana, *Chem. Mater.*, **13** (5), 1905-09 (2001).
- [15] M. Kakihana, *J. Sol.-Gel Sci. Technol.*, **6**, 7-55. (1996).
- [16] V. Caciuc, A. V. Postnikov and G. Borstel, *Phys. Rev. B.*, **61**, 8806-13 (2000).
- [17] A. Lorenzo, H. Loro, J. E. Munoz Santiuste, M. C. Terrile, G. Boulon, L. E. Bausa and J. Garcia Sole, *Opt. Mater.*, **8**, 55-63 (1997).

(Received December 20, 2002; Accepted February 3, 2003)